# Asymmetric Magnetic Reconnection in the Solar Atmosphere

Nick Murphy

Harvard-Smithsonian Center for Astrophysics

PPPL Theory Seminar
August 29, 2013

*Collaborators and Co-Conspirators:* John Raymond, Kathy Reeves, Mari Paz Miralles, Chengcai Shen, Jun Lin, Lei Ni, Carl Sovinec, Jake King, Clare Parnell, Andrew Haynes, Trae Winter, Yingna Su, Mitsuo Oka, Lijia Guo, Yi-Min Huang, Slava Lukin, Paul Cassak, Aleida Young, Drake Ranquist, and Crystal Pope

# Outline

- Background information
  - Asymmetric magnetic reconnection
  - Standard model of solar flares
- Recent results
  - Observational signatures of asymmetric reconnection in solar flares and coronal mass ejections (CMEs)
  - The plasmoid instability during asymmetric inflow reconnection
  - What does it mean for a magnetic null point to move?

# Introduction

- Most models of reconnection assume symmetry
- However, asymmetric magnetic reconnection occurs in the solar atmosphere, solar wind, space/astrophysical plasmas, and laboratory experiments
- *Asymmetric inflow reconnection* occurs when the upstream magnetic fields and/or plasma parameters differ
  - Earth's dayside magnetopause
  - Tearing in tokamaks, RFPs, and other confined plasmas
  - Solar jets
  - 'Pull' reconnection in MRX
- *Asymmetric outflow reconnection* occurs when conditions in the outflow regions are different
  - Solar flare and CME current sheets
  - Earth's magnetotail
  - Spheromak merging
  - 'Push' reconnection in MRX

# Cassak & Shay (2007) consider the scaling of asymmetric inflow reconnection

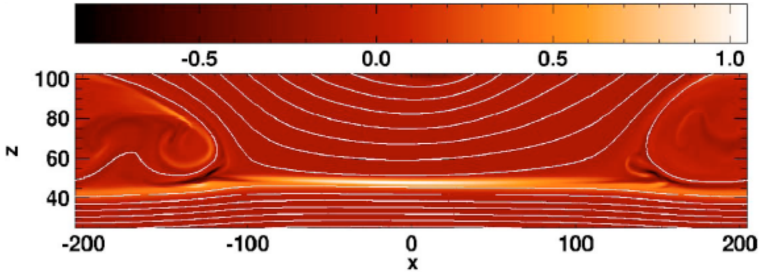


- Assume Sweet-Parker-like reconnection with different upstream magnetic fields $(B_L, B_R)$ and densities $(\rho_L, \rho_R)$
- The outflow velocity scales as a hybrid Alfvén velocity:

$$V_{out} \sim V_{Ah} \equiv \sqrt{\frac{B_L B_R \left(B_L + B_R\right)}{\rho_L B_R + \rho_R B_L}} \qquad (1)$$

- The X-point and flow stagnation point are not colocated

# Flux rope models of CMEs predict a current sheet behind the rising flux rope

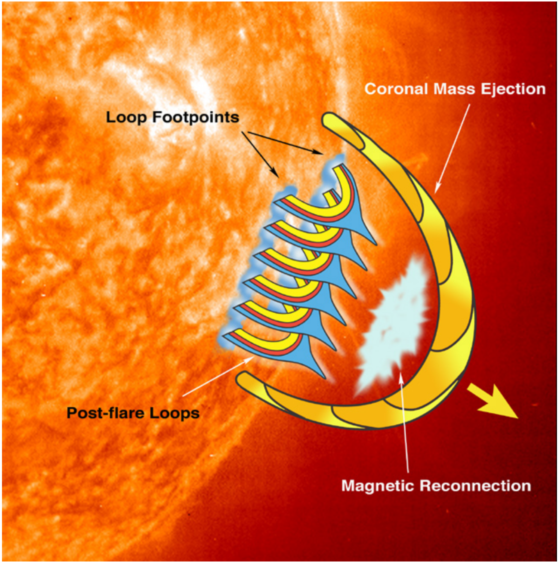


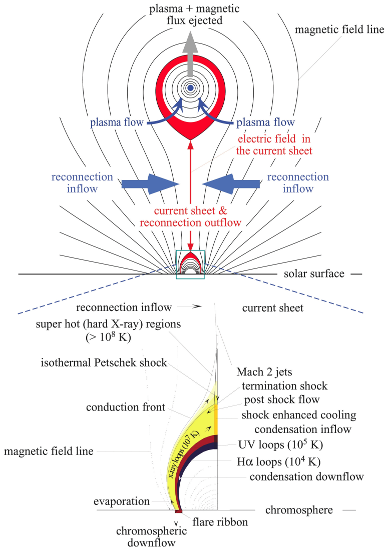

# A signature of reconnection: 'current sheet' structures

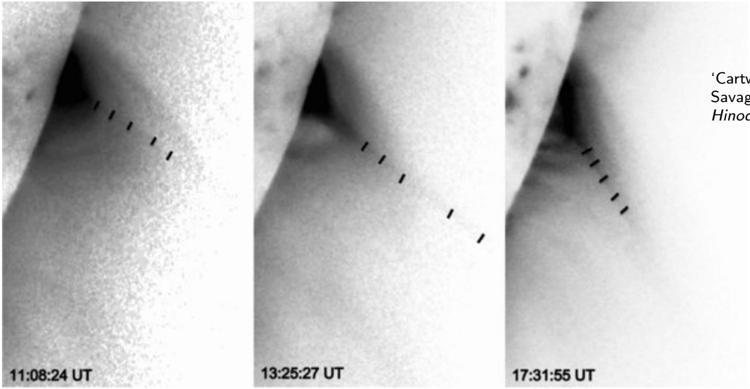


'Cartwheel CME'
Savage et al. (2010)
*Hinode*/XRT

- White light, X-ray, and EUV observations show sheet-like structures between the flare loops and the rising flux rope
- Much thicker than expected; the current sheet may be embedded in a larger-scale plasma sheet
- Current sheets sometimes drift considerably → asymmetry?
- Key limitation: lack of coronal magnetic field diagnostics

# How does magnetic asymmetry impact the standard model of solar flare reconnection?

- Observational signatures of the standard model include:
  - Ray-like structures (observed in X-rays, EUV, white light)
  - Inflows/outflows
  - Flare loops
    - Hard X-ray emission at loop footpoints where nonthermal particles hit chromosphere
    - Apparent motion of footpoints of newly reconnected loops away from each other
- We perform resistive MHD simulations of line-tied asymmetric reconnection using NIMROD (Murphy et al. 2012)
  - Initial X-line perturbation near wall representing photosphere for Harris-like configuration with $B_L/B_R \in \{0.125, 0.25, 0.5, 1\}$

$$B_y(x) = \frac{B_0}{1+b} \tanh\left(\frac{x}{\delta_0} - b\right) \tag{2}$$

  - Caveats: $\beta$ larger than reality for force balance, unphysical upper wall BC, no vertical stratification/3D effects

# The X-point is low so most released energy goes up

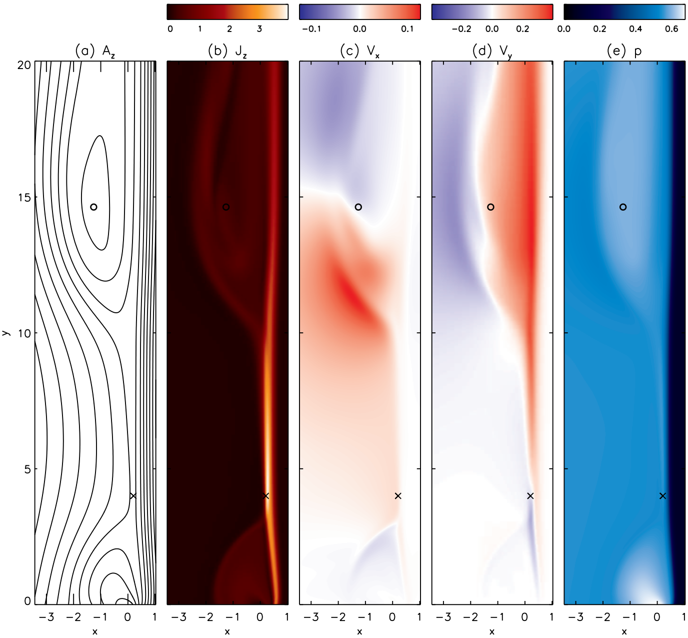


$$\frac{B_L}{B_R} = 0.25$$
$$V_{Ah} = 0.5$$

# There is significant plasma flow across the X-line in both the inflow and outflow directions (see also Murphy 2010)

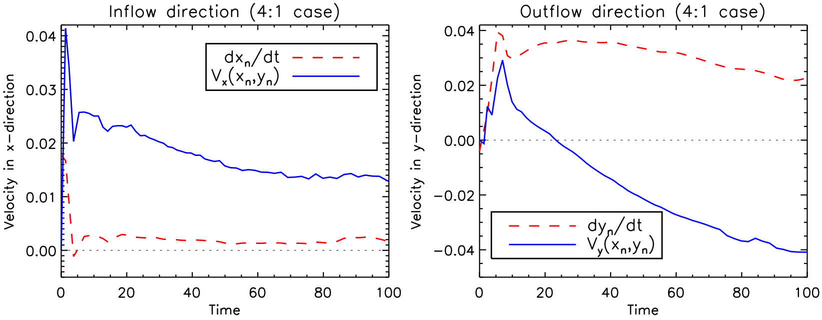


- $V_x(x_n, y_n)$ and $V_y(x_n, y_n)$ give the flow velocity at the X-line
- $\mathrm{d}x_n/\mathrm{d}t$ and $\mathrm{d}y_n/\mathrm{d}t$ give the rate of X-line motion
- For $t \gtrsim 25$, the X-line moves upward *against* the bulk flow

# The flare loops develop a skewed candle flame shape

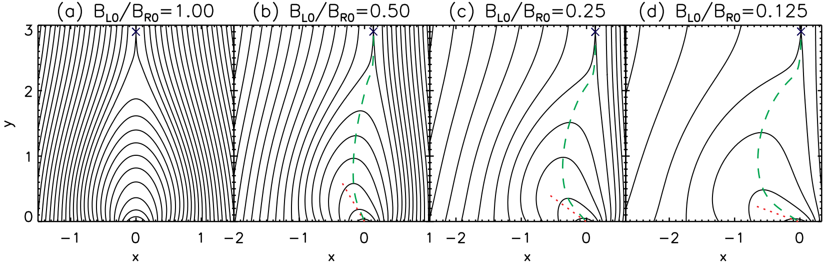


- Dashed green line: loop-top positions
- Dotted red line: analytic asymptotic approximation

# The Tsuneta (1996) flare is a famous candidate event

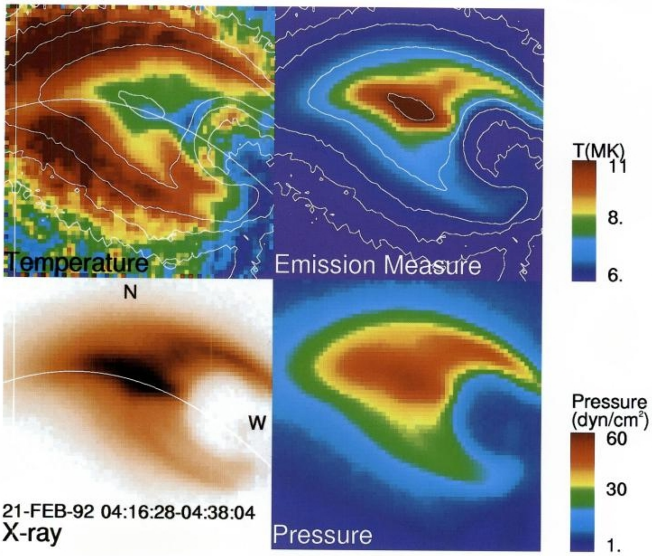


- Shape suggests north is weak **B** side

# We fit simulated loops to multi-viewpoint observations to constrain the magnetic asymmetry

Solar Dynamics Observatory

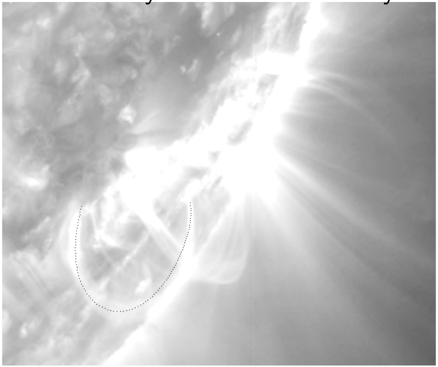

STEREO A

With D. Ranquist and M. P. Miralles

- The most important constraints are
  - Location of looptop relative to footpoints
  - Different perspectives from *STEREO A/B* and *SDO*
- Results for two events: asymmetries between 1.5 and 4.0

# Asymmetric speeds of footpoint motion

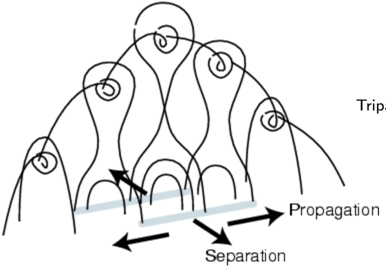


Tripathi et al. (2006)

- The footpoints of newly reconnected loops show apparent motion away from each other as more flux is reconnected
- Equal amounts of flux reconnected from each side
  $\Rightarrow$ Weak **B** footpoint moves faster than strong **B** footpoint
- Because of the patchy distribution of flux on the photosphere, more complicated motions frequently occur

# Asymmetric hard X-ray (HXR) footpoint emission

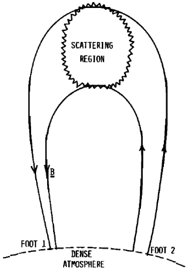


Melrose & White (1979, 1981)

- HXR emission at flare footpoints results from energetic particles impacting the chromosphere
- Magnetic mirroring is more effective on the strong **B** side
- More particles should escape on the weak **B** side, leading to greater HXR emission
- This trend is observed in $\sim 2/3$ of events (Goff et al. 2004)

# The outflow plasmoid develops net vorticity because the reconnection jet impacts it obliquely rather than directly

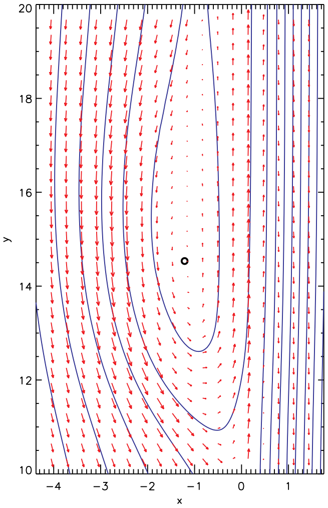


- Velocity vectors in reference frame of O-point
- Rolling motion observed in many prominence eruptions

# Take away points

- Magnetic asymmetry leads to observational consequences during solar reconnection
  - Flare loops with skewed candle flame shape
  - Asymmetric footpoint motion and hard X-ray emission
  - Drifting of current sheet into strong field region
  - Rolling motions in rising flux rope
- Important effects not included in these simulations:
  - Realistic 3D magnetic geometry
  - Patchy distribution of photospheric flux
  - Vertical stratification of atmosphere
  - Collisionless effects
- Comparing to observation is needed to understand 3D effects
  - Need to systematically investigate multiple signatures together and test falsifiable hypotheses
- Next topic: plasmoid instability during asymmetric inflow reconnection

# Elongated current sheets are susceptible to the plasmoid instability (Loureiro et al. 2007)

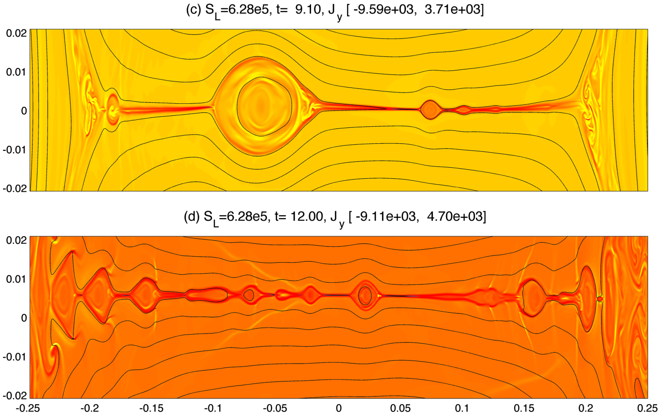


Bhattacharjee et al. (2009)
Huang et al. (2010–2013)

- The reconnection rate levels off at $\sim$0.01 for $S \gtrsim 4 \times 10^4$
- Shepherd & Cassak (2010) argue that this instability creates small enough structures for collisionless reconnection to onset
- CME current sheet blobs may be plasmoids (Guo et al. 2013)

# What are the dynamics of the plasmoid instability during asymmetric inflow reconnection?

- Most simulations of the plasmoid instability assume reconnection with symmetric upstream fields
  - Simplifies computing and analysis
  - Plasmoids and outflows interact in one dimension
- In 3D, flux ropes twist and writhe and sometimes bounce off each other instead of merging
  - Asymmetric simulations offer clues to 3D dynamics
- We perform NIMROD simulations of the plasmoid instability with asymmetric magnetic fields (Murphy et al. 2013)
  - (Hybrid) Lundquist numbers up to $10^5$
  - Two initial X-line perturbations along $z = 0$
  - $B_L/B_R \in \{0.125, 0.25, 0.5, 1\}$; $\beta_0 \geq 1$; periodic outflow BCs

# Plasmoid instability: symmetric inflow ($B_{L0}/B_{R0} = 1$)

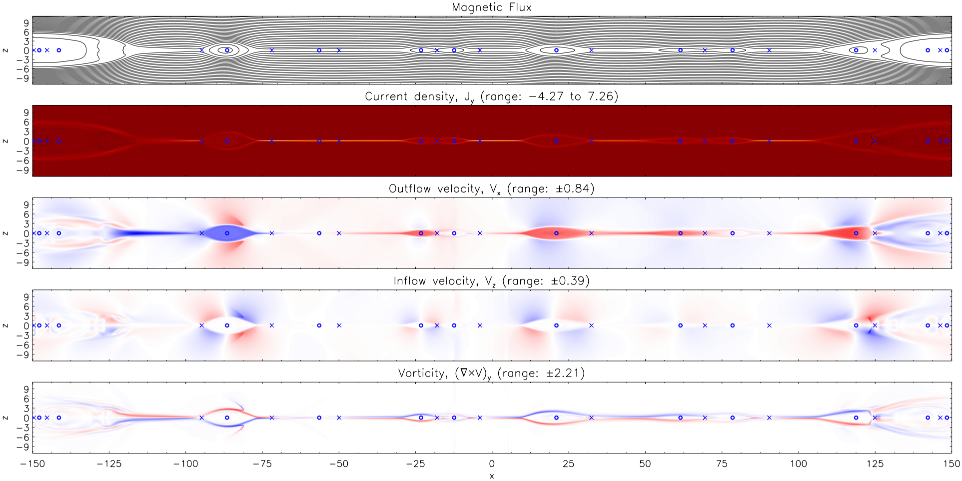


- X-points and O-points are located along symmetry axis
- X-points often located near one exit of each current sheet
- No net vorticity in islands

# Plasmoid instability: asymmetric inflow ($B_{L0}/B_{R0} = 0.25$)

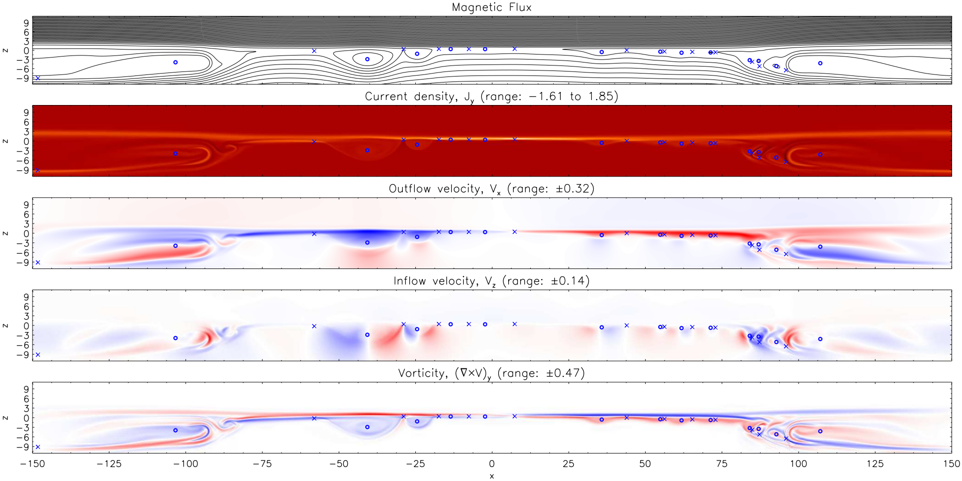


- Displacement between X-point and O-points along $z$ direction
- Islands develop preferentially into weak field upstream region
- Islands have vorticity and downstream regions are turbulent

# Secondary merging is doubly asymmetric

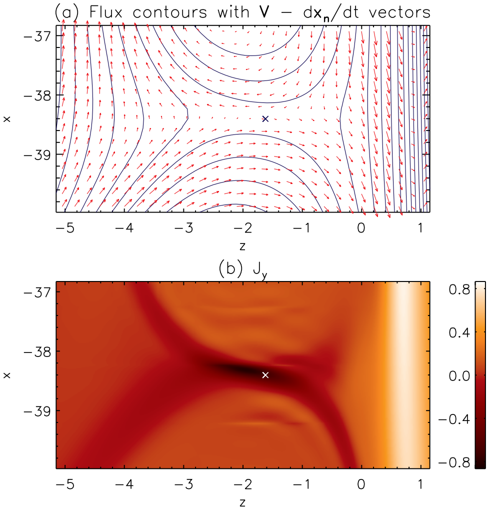


- Bottom island is much larger $\Rightarrow$ island merging is not head-on
- Flow pattern dominated by shear flow associated with island vorticity $\Rightarrow$ Partial stabilization of secondary reconnection

# What insights do these simulations provide for the 3D plasmoid instability?

- Daughton et al. (2011): plasmoids in 3D will be complicated flux rope structures
- Outflow jets will generally impact flux ropes obliquely
  - Momentum transport from outflow jets to flux ropes may be less efficient
  - Merging between colliding flux ropes may be incomplete due to flux rope vorticity
- Questions that keep me awake at night:
  - How does the plasmoid instability behave in 3D?
  - What is the 3D reconnection rate?
  - How do reconnection sites interact in 3D?
  - What mistakes are we making by using 2D simulations to interpret fundamentally 3D behavior?
  - How will these effects change statistical models of islands?
- Final topic: motion of magnetic null points

# What does it mean for a magnetic null point to move?

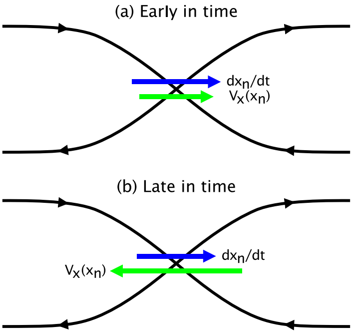


- In these simulations, the nulls move at velocities different from the plasma flow velocity: $\frac{\mathrm{d}\mathbf{x}_n}{\mathrm{d}t} \neq \mathbf{V}(\mathbf{x}_n)$
  - Gap between flow stagnation point and magnetic field null
  - Plasma flow and X-line motion often in different directions
- To understand this, we derive an exact expression describing the motion of an isolated null point
  - We consider isolated null points because null lines and null planes are structurally unstable in 3D

# Definitions

- The time-dependent position of an isolated null point is

$$\mathbf{x}_n(t) \tag{3}$$

- The null point's velocity is:

$$\mathbf{U} \equiv \frac{\mathrm{d}\mathbf{x}_n}{\mathrm{d}t} \tag{4}$$

- The Jacobian matrix of the magnetic field at the null point is

$$\mathbf{M} \equiv \left( \begin{array}{ccc} \partial_x B_x & \partial_y B_x & \partial_z B_x \\ \partial_x B_y & \partial_y B_y & \partial_z B_y \\ \partial_x B_z & \partial_y B_z & \partial_z B_z \end{array} \right)_{\mathbf{x}_n} \tag{5}$$

# We derive an expression for the motion of a null point in an arbitrary time-varying vector field with smooth derivatives

- First we take the derivative of the magnetic field following the motion of the magnetic field null,

$$\left.\frac{\partial \mathbf{B}}{\partial t}\right|_{\mathbf{x}_n} + \left.(\mathbf{U} \cdot \nabla)\,\mathbf{B}\right|_{\mathbf{x}_n} = 0 \tag{6}$$

  The RHS equals zero because the magnetic field will not change from zero as we follow the null point.

- By solving for $\mathbf{U}$ in Eq. 6, we arrive at the exact relation

$$\mathbf{U} = -\mathbf{M}^{-1} \left.\frac{\partial \mathbf{B}}{\partial t}\right|_{\mathbf{x}_n} \tag{7}$$

  - Independent of Maxwell's equations
  - Assumes $C^1$ continuity of $\mathbf{B}$ about $\mathbf{x}_n$
  - Unique, well-defined velocity when $\mathbf{M}$ is non-singular

# We use Faraday's law to get an expression for the motion of a null point that remains independent of Ohm's law

- Faraday's law is given exactly by

$$\frac{\partial \mathbf{B}}{\partial t} = -\nabla \times \mathbf{E} \tag{8}$$

- By applying Faraday's law to Eq. 7, we arrive at

$$\mathbf{U} = \mathbf{M}^{-1} \ \nabla \times \mathbf{E}\big|_{\mathbf{x}_n} \tag{9}$$

# In resistive MHD, null point motion results from a combination of advection by the bulk plasma flow and resistive diffusion of the magnetic field

- Next, we apply the resistive MHD Ohm's law,

$$\mathbf{E} + \mathbf{V} \times \mathbf{B} = \eta \mathbf{J} \tag{10}$$

  where we assume the resistivity to be uniform.

- The expression for the rate of motion of a null point becomes

$$\mathbf{U} = \mathbf{V} - \eta \, \mathbf{M}^{-1} \, \nabla^2 \mathbf{B} \tag{11}$$

  where all quantities are evaluated at the magnetic null point. The terms on the RHS represent null point motion by
  - Bulk plasma flow
  - Resistive diffusion of the magnetic field

# Murphy (2010): 1D X-line retreat via resistive diffusion

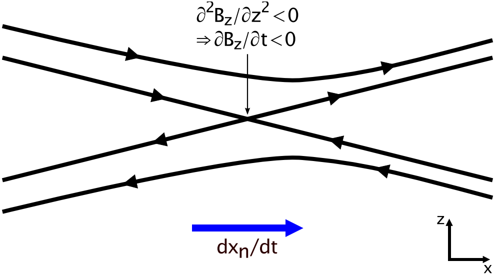


- $B_z$ is negative above and below the X-line
- Diffusion of $B_z$ leads to the current X-line position having negative $B_z$ at a slightly later time
- The X-line moves to the right as a result of diffusion of the normal component of the magnetic field

$$\frac{\mathrm{d}x_n}{\mathrm{d}t} = V_x(x_n) - \eta \left[ \frac{\frac{\partial^2 B_z}{\partial x^2} + \frac{\partial^2 B_z}{\partial z^2}}{\frac{\partial B_z}{\partial x}} \right]_{x_n} \tag{12}$$

# What does it mean for a magnetic null point to move?

- The velocity of a null point depends intrinsically on *local* plasma parameters evaluated at the null
- Global dynamics help set the local conditions
- A unique null point velocity exists if $\mathbf{M}$ is non-singular
- Nulls are not objects and cannot be pushed by, e.g., pressure gradient forces
  - Indirect coupling between the momentum equation and the combined Faraday/Ohm's law
  - Plasma not permanently affixed to nulls in non-ideal cases
- How do we connect this local expression into global models?

# Appearance and disappearance of null points

- In resistive MHD, nulls must diffuse in and out of existence
  - Not accounted for in bifurcation theory/topological analysis
- At instant of formation, a null is degenerate
  - The Jacobian $\mathbf{M}$ is singular
- Bifurcating null-null pairs will go in the directions along which $\mathbf{B}$ and $\frac{\partial \mathbf{B}}{\partial t}$ have opposite sign
- The instantaneous velocity of separation is infinite

## Can we perform a similar local analysis to describe the motion of separators?

- A separator is a magnetic field line connecting two null points
  - These are often important locations for reconnection.
- Suppose that there is non-ideal behavior only along one segment of a separator.
- At a slightly later time, the field line in the ideally evolving region will in general no longer be the separator, even though the evolution was locally ideal
- Therefore, it is not possible to find an exact expression describing separator motion based solely on local parameters.
- However, a global approach could lead to an exact expression by taking into account connectivity changes along the separator as well as motion of its endpoints.

# Conclusions

- Magnetic asymmetry during solar eruptions lead to observational consequences
  - Flare loops have a skewed candle flame shape
  - Asymmetric footpoint motion and hard X-ray emission
  - Drifting of current sheet into strong field region
  - Rolling motions in rising flux rope
- Magnetic asymmetry qualitatively changes the dynamics of the plasmoid instability
  - Islands develop into weak field upstream region
  - Jets impact islands obliquely $\Rightarrow$ net vorticity
  - Secondary merging is less efficient
- We derive an exact expression to describe the motion of magnetic field lines
  - The motion of magnetic null point depends on parameters evaluated at the null
  - Null point motion in resistive MHD is caused by bulk plasma flow and diffusion of the component of $\mathbf{B}$ orthogonal to the motion

# Ongoing and Future Work

- HiFi simulations of reconnection in partially ionized chromospheric plasmas (with Slava Lukin)
  - Effects of asymmetry?
  - Does chromospheric reconnection lead to elemental fractionation?
- Non-equilibrium ionization modeling of coronal mass ejection plasma (e.g., Murphy et al. 2011) and current sheets (e.g., Shen et al. 2013)
- Eigenmode analysis of asymmetric plasmoid instability to get linear properties (with Yi-Min Huang)
- Analytic expression for the motion of separators
  - On my "to do" list for 2016.